International Journal of Digital Earth

ISSN: (Print) (Online) Journal homepage: https://www.tandfonline.com/loi/tjde20

# Machine learning methods' performance in radiative transfer model inversion to retrieve plant traits from Sentinel-2 data of a mixed mountain forest

Abebe Mohammed Ali , Roshanak Darvishzadeh , Andrew Skidmore , Tawanda W. Gara & Marco Heurich

**To cite this article:** Abebe Mohammed Ali , Roshanak Darvishzadeh , Andrew Skidmore , Tawanda W. Gara & Marco Heurich (2020): Machine learning methods' performance in radiative transfer model inversion to retrieve plant traits from Sentinel-2 data of a mixed mountain forest, International Journal of Digital Earth, DOI: 10.1080/17538947.2020.1794064

**To link to this article:** https://doi.org/10.1080/17538947.2020.1794064



Published online: 15 Jul 2020.

INTERNATIONAL JOURNAL OF DIGITAL EARTH
https://doi.org/10.1080/17538947.2020.1794064



# Machine learning methods' performance in radiative transfer model inversion to retrieve plant traits from Sentinel-2 data of a mixed mountain forest

Abebe Mohammed Ali [a,b], Roshanak Darvishzadeh [a], Andrew Skidmore [a,c], Tawanda W. Gara [a,d] and Marco Heurich [e,f]

[a]Faculty of Geo-Information Science and Earth Observation (ITC), University of Twente, Enschede, The Netherlands; [b]Department of Geography and Environmental Studies, Wollo University, Dessie, Ethiopia; [c]Department of Environmental Science, Macquarie University, Sydney, Australia; [d]Department of Geography and Environmental Science, University of Zimbabwe, Harare, Zimbabwe; [e]Department of Visitor Management and National Park Monitoring, Bavarian Forest National Park, Grafenau, Germany; [f]Chair of Wildlife Ecology and Wildlife Management, University of Freiburg, Freiburg, Germany

**ABSTRACT**

Assessment of vegetation biochemical and biophysical variables is useful when developing indicators for biodiversity monitoring and climate change studies. Here, we compared a radiative transfer model (RTM) inversion by merit function and five machine learning algorithms trained on an RTM simulated dataset predicting the three plant traits leaf chlorophyll content (LCC), canopy chlorophyll content (CCC), and leaf area index (LAI), in a mixed temperate forest. The accuracy of the retrieval methods in predicting these three plant traits with spectral data from Sentinel-2 acquired on 13 July 2017 over Bavarian Forest National Park, Germany, was evaluated using *in situ* measurements collected contemporaneously. The RTM inversion using merit function resulted in estimations of LCC ($R^2 = 0.26$, RMSE = 3.9 μg/cm$^2$), CCC ($R^2 = 0.65$, RMSE = 0.33 g/m$^2$), and LAI ($R^2 = 0.47$, RMSE = 0.73 m$^2$/m$^2$), comparable to the estimations based on the machine learning method Random forest regression of LCC ($R^2 = 0.34$, RMSE = 4.06 μg/cm$^2$), CCC ($R^2 = 0.65$, RMSE = 0.34 g/m$^2$), and LAI ($R^2 = 0.47$, RMSE = 0.75 m$^2$/m$^2$). Several of the machine learning algorithms also yielded accuracies and robustness similar to the RTM inversion using merit function. The performance of regression methods trained on synthetic datasets showed promise for fast and accurate mapping of plant traits accross different plant functional types from remote sensing data.

**ARTICLE HISTORY**
Received 31 March 2020
Accepted 6 July 2020

**KEYWORDS**
Leaf area index; leaf/canopy chlorophyll content; radiative transfer model; look-up table; machine learning algorithms

## 1. Introduction

The assessment of plant functional diversity at ecosystem level is mainly addressed by examining dynamic processes and evaluating plant traits (Gamon et al. 2019). Leaf traits and biophysical characteristics are essential indicators in monitoring and assessing the functioning and structure of terrestrial ecosystem biodiversity (Pereira et al. 2013; Skidmore et al. 2015). Traits such as leaf

**CONTACT** Abebe Mohammed Ali abebemohammed@yahoo.co.uk Faculty of Geo-Information Science and Earth Observation (ITC), University of Twente, P.O. Box 217, Enschede 7500 AE, The Netherlands Department of Geography and Environmental Studies, Wollo University, P.o box 1145, Dessie, Ethiopia

chlorophyll content (LCC), canopy chlorophyll content (CCC) and leaf area index (LAI) have been long used in ecological and climate studies as input to biospheric models for the prediction of surface energy balance and primary productivity, as well as the assessment of plant health conditions and $CO_2$ exchange rates (Myneni et al. 1997). Measurement of these traits based on field observations at different spatiotemporal scales is labour-intensive and time-consuming. Remote sensing could play a critical role by acquiring such data over broad spatial scales (Wang et al. 2010). The advancement in remote sensing sensors regarding spatial, temporal and spectral resolutions enables us to accurately measure fundamental plant traits using remote sensing data at local, regional, and global level (Houborg, Fisher, and Skidmore 2015).

The Sentinel-2 multispectral imager is a constellation with two twin satellites, Sentinel-2A and Sentinel-2B, that can be used to quantify biodiversity variables (Drusch et al. 2012). The efficient production of high-quality plant trait maps from Sentinel-2 data requires evaluating the performance of existing methods and developing new ones. Although many studies quantified different plant traits using remote sensing data in the past four decades, to our knowledge, few studies have assessed the retrieval of chlorophyll and LAI using Sentinel-2 data. Darvishzadeh et al. (2019) retrieved LCC of a temperate forest through radiative transfer model (RTM) inversion, and Ali et al. (2020) compared existing empirical and RTM inversion methods for predicting CCC from Sentinel-2 data. Also, vegetation indices optimized for Sentinel-2 were used for the estimation of crop LAI and chlorophyll content (e.g. Clevers, Kooistra, and van den Brande 2017; Pasqualotto et al. 2019).

Popular techniques commonly used for prediction of plant traits and vegetation biophysical characteristics from remotely sensed data are generally categorized as statistical-based, physically-based (radiative transfer models), and hybrid approaches. The statistical-based approaches are parametric or non-parametric regression models that relate the variable(s) of interest to the remote sensing spectral data or their derivative (e.g. vegetation indices) (Skidmore 2002; Darvishzadeh et al. 2008b; Atzberger et al. 2015). Vegetation indices are widely used to enhance the relationship between a variable of interest and spectral data by utilizing only the most informative spectral feature, and thus minimizing the effect of confounding factors such as topography, soil background and atmospheric effects (Asner 1998; Thenkabail, Smith, and De Pauw 2000; Broge and Mortensen 2002; Darvishzadeh et al. 2008a). There are a number of regression models (also commonly known as statistical machine learning methods) in the literature that can be used to establish empirical relationships between the variable of interest (e.g. chlorophyll, LAI) and remote sensing spectral data, either directly through its derivatives, or using vegetation indices for accurate prediction. The broadly used statistical machine learning methods include linear non-parametric models such as Stepwise multiple linear regression (SMLR), Principal components regression (PCR), Partial least squares regression (PLSR) and Ridge (regulated) regression (RR), and non-linear non-parametric regression methods such as decision tree learning (e.g. random forest regression (RFR)), Artificial neural networks (ANNs), Kernel methods (e.g. support/relevance vector machines (SVM), and kernel ridge regression (KRR)), Gaussian Process Regression (GPR), and Bayesian networks (Verrelst et al. 2015; Féret et al. 2018; Holloway and Mengersen 2018).

Statistical models are easy to apply and are readily available; thus, they are extensively used. However, statistical models developed for a specific site or sensor configuration lack transferability to other locations with different vegetation types, to other sensor configurations, or to different times of data acquisition (Vuolo et al. 2013). Their major pitfall emanates from their need for *in situ* datasets for training and validation. The number, quality, and representativeness of the *in situ* datasets determine the robustness of statistical models. Hence, a thorough test of the accuracy and robustness of these predictive models depends on large data volumes and variability, which is challenging and may lead to high costs being incurred when trying to obtain such data based on merely *in situ* measurements.

The alternative is to use physical-based approaches, which allow simulating a large dataset that can be used for training of the statistical models, thus reducing the dependency on field data or inversion procedures to retrieve variables of interest. The physical approach involves the use of RTMs.

RTMs simulate the surface reflectance that can be recorded by a sensor as a function of leaf properties, canopy structure (e.g. crown shape, forest stand density, and canopy heterogeneity), sensor configuration, illumination geometry, and background (Houborg, Soegaard, and Boegh 2007; Jacquemoud et al. 2009). A large variety of canopy RTMs are currently available ranging from the one-dimensional or turbid media models (e.g. Scattering by Arbitrarily Inclined Leaves (SAIL) model) that assume horizontally homogeneous canopy structure (Huemmrich 2001) to Monte Carlo ray tracing three-dimensional (3D) models (e.g. Discrete anisotropic radiative transfer (DART) model), which simulate reflectance by stochastically calculating photon trajectories within turbid or geometric canopies. For more information, an inter-comparison of canopy RTM models is reported by Widlowski et al. (2015).

Complex models seem to be more realistic, but they have many variables and are therefore hard to parameterize and invert, whereas simpler models may be less realistic but easier to invert (Verrelst et al. 2015). Nevertheless, a study by Yanez-Rausell et al. (2015) demonstrated the comparable performance of the computationally less intensive RTM-PARAS with the DART 3D model. PARAS uses a simplified forest structural description, whereas DART uses a detailed 3D structural forest parametrization coupled with a leaf radiative transfer model. Therefore, less intensive hybrid models, such as the Invertible Forest Reflectance model (INFORM) (Schlerf and Atzberger 2006), which is a combination of the forest light interaction model (Rosema et al. 1992) and SAIL (Verhoef 1984) canopy RTMs with the leaf PROSPECT (property spectra) model (Jacquemoud and Baret 1990) RTM, seem to be particularly suitable and is the choice to be tested in this study.

The inversion of a canopy RTM is considered to be a physically sound approach for the retrieval of bio-geophysical variables of terrestrial surfaces because the approach is generic and therefore has more general applicability and transferability (Malenovský et al. 2008; Verrelst et al. 2010; Féret et al. 2011; Atzberger et al. 2013). Inversion of an RTM can be performed using techniques such as look-up table (LUT) inversion, iterative numerical optimization methods, or hybrid approaches (Verrelst et al. 2015) in which RTMs are used to simulate data for input to train machine learning regression methods. LUT inversion of RTMs by using merit functions is computationally demanding and may not be operationally feasible for large scale mapping.

Therefore, combining the generic capabilities of physically-based methods with flexible and computationally efficient statistical methods, such as machine learning approaches, may best suit large-scale mapping of plant traits. RTMs are used to simulate canopy reflectance based on the spectral band specifications and configurations of a sensor, and are used to train parametric or non-parametric regression methods to link spectral information and canopy parameters (Jacquemoud et al. 2009). These hybrid inversion methods have the advantage of empirical method simplicity in addition to physical model universality, while being able to estimate the properties of vegetation accurately and quickly (Verrelst et al. 2015). A considerable amount of literature has been published on the performance of such hybrid methods. Liang et al. (2016) compared the performance of three hybrid methods namely curve-fitting, least squares support vector regression (LS-SVR) and RFR algorithms for LCC and CCC retrieval, by using simulated Compact High-Resolution Imaging Spectrometer (CHRIS) datasets that were generated by the SAIL coupled with PROSPECT (PROSAIL) radiative transfer model in crop fields. Their validation result demonstrated RFR to be the optimal method for their modelling. Baret (2016) implemented ANN trained on PROSAIL simulated data for regional and global prediction of biophysical variables, including CCC from Sentinel-2; their algorithm is also implemented in the ESA Sentinel application platform toolbox. Retrieval of forest leaf functional traits from HySpex imagery using the INFORM radiative transfer models inversion and stepwise multilinear regression was evaluated by Ali et al. (2016b). Atzberger et al. (2015) compared LUT based inversion of the PROSAIL RTM to second-order polynomial function, fitted on wavelengths reflectance and vegetation indices calculated from the synthetic data, to retrieve LAI in Mediterranean grassland from airborne imaging spectroscopy. To date, there has been little agreement on which machine learning algorithm to implement for large scale mapping of plant traits.

To the best of our knowledge, there have been no detailed studies assessing the accuracy of different machine learning regression methods calibrated on RTM generated synthetic data to retrieve multiple plant traits in a forest ecosystem. By evaluating the accuracy of the overarching machine learning approaches available in the literature, we aim to increase the predictive power and robustness of RTM inversions in the forest by combining the advantages of physical and statistical-based models. With the objective to derive a fast and efficient RTM inversion scheme for predicting plant traits in a forest ecosystem from freely available spaceborne data, this study presents a comparative accuracy assessment of the results from five machine learning methods as well as LUT using the merit function approach for the INFORM inversion on Sentinel-2 data to predict the plant traits LCC, CCC and LAI in a mixed mountain forest.

## 2. Materials and methods

### 2.1. Study area

The test site for this study was the Bavarian Forest National Park (BFNP) in south-eastern Germany, with the centre coordinates 13°12′9″ E (longitude) and 49°3′19″ N (latitude), along the border to the Czech Republic. The BFNP has a mixed mountain forest with an approximate area of 240 $km^2$ and a temperate climate. Elevation varies from 600 m to 1453 m. Annual precipitation ranges from 1,200 mm to 1,800 mm, with annual temperature averages from 3° to 6° Celsius (Heurich et al. 2010).

The BFNP has valley, hillside, and highland ecological zones. Alluvial spruce forests are dominant in the valleys, mixed mountain forests are found on the hillsides and mountain spruce forests in the high areas (Heurich et al. 2010). European beech (Fagus sylvatica), Norway Spruce (Picea abies) and Fir (Abies alba) are the three dominant tree species. Sycamore Maple (Acer pseudoplatanus L), Mountain Ash (Sorbus aucuparia L), and Goat Willow (Salix caprea) are infrequently found in deciduous stands in the park (Cailleret, Heurich, and Bugmann 2014). Due to massive disturbance by bark beetles and wind storms in recent decades, the forest structure in the BFNP is very heterogeneous (Lehnert et al. 2013).

### 2.2. Data

#### 2.2.1. In situ data

The field measurements were collected in July 2017. The study area was stratified into conifer, broadleaf, and mixed stands, and a random sampling technique was implemented to collect samples in each stratum. Biophysical and biochemical variables were obtained in total from 32 square plots with 30 m sides. Geographic coordinates of the plots were recorded at the centre using a handheld Garmin Global Positioning System (GPS) that has a geometric accuracy of ±5 m. The structural variable LAI was measured using Li-Cor LAI-2200 canopy analyzer equipment for each sample plot. We followed a similar procedure of taking one reference (above the canopy) reading in the nearest open field, and five below canopy measurements inside each plot in estimating LAI as described in Darvishzadeh et al. (2019). A maximum effort was made to take the LAI-2200 measurements with constant illumination conditions for the above and below canopy readings.

In each plot, a crossbow was used to collect sample leaves/shoots/needles from the mature sunlit part of the top of the canopy (Ali et al. 2016a). These samples were collected from two to three branches of the representative trees in each plot. Their chlorophyll content was immediately measured using a Chlorophyll Content Meter (CCM-300) and weighed average by species biomass to determine leaf chlorophyll content per plot (see Gara et al. (2019) for details). The CCC of each plot was calculated by multiplying the plot's average LCC and LAI. The summary of these field measurements is presented in Table 1.

**Table 1.** Basic statistics of the *in situ* measured variables: leaf chlorophyll content (LCC), leaf area index (LAI), and canopy chlorophyll content (CCC).

| Summary | LCC (μg $cm^{-2}$) | LAI ($m^2$ $m^{-2}$) | CCC (g $m^{-2}$) |
|---|---|---|---|
| Minimum | 33.62 | 1.33 | 0.58 |
| Maximum | 51.75 | 5.4 | 2.42 |
| Mean | 42.80 | 3.82 | 1.62 |
| Std.dev | 4.83 | 1.01 | 0.46 |

#### 2.2.2. Sentinel-2 data and pre-processing

The cloud-free Sentinel-2A image of the study area generated on 13 July 2017 was used to study the three plant traits further. The Sentinel-2A level 1c product was downloaded from the ESA Copernicus open access hub (https://scihub.copernicus.eu). Top-of-atmosphere (TOA) reflectance (level 1c product) was processed into top-of-canopy (TOC) reflectance (level 2A product) and resampled to a 20 m spatial resolution using Sen2cor 2.5.5 stand-alone software, which is freely distributed under the GNU general public license (http://step.esa.int/main/third-party-plugins-2/sen2cor). Spectral information from ten bands (bands 2, 3, 4, 5, 6, 7, 8, 8a, 11, and 12) was utilized in this study. The remaining three bands at 443, 945, and 1374 nm central wavelength (bands 1, 9, and 10, respectively) serve mainly for atmospheric correction and were not relevant for our purpose. The TOC reflectance data of the pixels containing the sample plots were extracted and used for validation of the performance of the different RTM inversion methods considered in predicting the three key plant variables.

### 2.3. Methods

#### 2.3.1. Physical based modelling

(a) *The INFORM radiative transfer model:* INFORM mimics forest canopy optical property with few input parameters compared to 3D RTMs (Atzberger 2000; Schlerf and Atzberger 2006). The capacity of INFORM to simulate forest spectra in forward mode was compared to other RTMs in Widlowski et al. (2015). Because of its simplicity and reliability in generating forest canopy synthetic spectra, we found this model to be a feasible choice for the purpose of forest canopy spectral simulation and as such it has successfully been inverted in several studies (e.g. Ali et al. 2016b; Wang et al. 2017; Darvishzadeh et al. 2019).

(b) *INFORM parameterization and LUT generation:* RT models offer a chance to simulate look-up tables (LUT) with large data volume and variability by incorporating a wide range of input parameters to ensure a thorough test of the accuracy and robustness of the inversion methods. The LUT should be extensive enough to achieve high accuracy (Combal et al. 2003) without becoming computationally too expensive. To determine LUT size requires a compromise between computation time and the accuracy of the prediction. Investigation and previous studies (e.g. Vuolo et al. 2010; Atzberger et al. 2015) led us to decide on a LUT size of 100,000 parameter combinations.

In this study, INFORM was coupled with PROSPECT-4 and its input parameters were four leaf and six canopy properties (Table 2), as well as sensor observation related parameters such as view zenith (θo), sun zenith (θs) and relative azimuth angle (Φ) to simulate top of canopy spectral reflectance of forest stands between the 400 and 2500 nm wavelengths. The ranges for input parameters were determined using prior knowledge from the field observations, literature review, and sensor configurations (Table 2). In INFORM, LAI is represented by single tree LAI (LAIs). Hence, LAIs was computed from LAI and canopy closure (CC) as in equation 1 (Schlerf and Atzberger 2006).

$$\mathrm{LAI_s} = \frac{\mathrm{LAI}}{\mathrm{CC}} \tag{1}$$

**Table 2.** INFORM input parameters used to generate the LUT and their ranges, as defined on the basis of literature review and sensor configuration (Sentinel-2 MSI).

| Parameter | Symbol | Unit | Range | | Source |
|---|---|---|---|---|---|
| | | | Min | Max | |
| Leaf dry mass per area | $C_m$ | g/cm$^2$ | 0.005 | 0.03 | Ali et al. (2016b) |
| Equivalent water thickness | $C_w$ | g/cm$^2$ | 0.006 | 0.035 | Ali et al. (2016b) |
| Leaf structural parameter | N | NA | 1 | 2.5 | Ali et al. (2016a) |
| Leaf chlorophyll content | LCC | µg/cm$^2$ | 20 | 65 | Field measurement |
| Single-tree LAI | $LAI_s$ | NA | 2 | 10 | Field measurement |
| Understory LAI | $LAI_u$ | NA | 0.2 | 1 | Field measurement |
| Stem density | SD | n/hr | 200 | 2000 | Ali et al. (2016b) |
| Stand height | SH | m | 5 | 40 | Ali et al. (2016b) |
| Crown diameter | CD | m | 3 | 10 | Ali et al. (2016b) |
| Average leaf angle | ALA | degree | 40 | 60 | Ali et al. (2016b) |
| Sun zenith angle | $\theta_s$ | degree | 25 | 35 | Image metadata |
| Observation zenith angle | $\theta_0$ | degree | 0 | 15 | Image metadata |
| Azimuth angle | $\Phi$ | degree | 50 | 210 | Image metadata |
| Scale | | NA | 0.5 | 1.5 | Schlerf and Atzberger (2006) |
| Fraction of diffused radiation | Sky1 | fraction | 0.1 | | Schlerf and Atzberger (2006) |

Note: Leaf and canopy level input parameter combinations were determined using a multivariate normal distribution function, whereas sensor configuration parameters were randomly distributed within their range.

High correlations among model input parameters have been reported in previous studies (e.g. Ali et al. 2016b). Hence, leaf and canopy level input parameter combinations were determined using a multivariate normal distribution function based on the mean and covariance matrix of their ground truth values. Sensor configuration parameters were randomly drawn within their range recorded in the metadata of the Sentinel-2 image, while others were fixed based on previous studies (Schlerf and Atzberger 2006; Ali et al. 2016b). Field spectra of understory vegetation and the forest floor elements were averaged and used as background reflectance during the simulation. The reliability of the INFORM model to simulate Sentinel-2 image data has been shown in Darvishzadeh et al. (2019) and was also checked here by comparing the INFORM simulated spectra of known samples obtained from Sentinel-2 TOC reflectance. A random Gaussian noise value of 0.3% was added to each simulated spectrum to account for model uncertainties.

### *2.3.2. INFORM inversion*

RTM inversions are considered generic and robust methods to estimate vegetation variables from remotely sensed data. The large data volume in an LUT can be used for a global search of a solution when inverted using merit functions. It also enables to train machine learning algorithms with sufficient samples and variability situations, thus improve the transferability of the algorithms.

In order to identify robust, accurate and reliable method(s) for the inversion of INFORM from Sentinel-2 data, this study evaluated six different retrieval algorithms using training data of 85% of the LUT generated by INFORM (85, 000 entries): (i) LUT inversion using a merit function, (ii) a linear non-parametric regression method (SMLR) and (iii) four non-linear non-parametric regression methods (ANN, GPR, RFR and SVM). The non-linear non-parametric methods were selected because of their ability to perform adaptively, nonlinear data fitting for the estimation of biophysical parameters from remote sensing data, and they are often used by the remote sensing community as powerful predictive methods (e.g. Verrelst et al. 2012; Baret 2016; Liang et al. 2016; Ali et al. 2016b). All analytical processes of the study were employed in Matlab (The Mathworks®). The execution time for each algorithm to train and predict the three traits over the whole study area was recorded. Descriptions of the simulation of training data using RTM and inversion methods are detailed in the following subsections.

Predictions of all methods were validated using the remaining 15% of the INFORM simulated dataset (15,000 entries) as well as the *in situ* measurements of the three variables as independent observations. The accuracy of the retrievals was portrayed using root mean square error (RMSE),

relative root mean square error (RRMSE), the coefficient of determination ($R^2$), and bias (Equations 2–5) between the *in situ* data and the predictions. A paired t-test was applied to discern whether the predictions were significantly different from the independent observations. Ranges and scatterplots were utilized to reveal the similarities and differences between the predictions and *in situ* measurements of the studied plant traits.

$$R^2 = 1 - \frac{\sum^{(y_i - y_i')} 2}{\sum^{(y_i - \overline{y_i})} 2} \tag{2}$$

$$\text{RMSE} = \sqrt{\frac{\sum^{(y_i - y'_i)} 2}{n}} \tag{3}$$

$$\text{RRMSE (\%)} = \sqrt{\frac{\sum^{(y_i - y'_i)} 2}{n}} / \overline{y_i} * 100 \tag{4}$$

$$\text{Bias} = \frac{\sum_i^y - y'_i}{n} \tag{5}$$

where $y_i$ and $y_i'$ are the actual and predicted values for sample $i$, $\overline{y_i}$ is the mean value of actual samples and n is the number of samples.

(a) *LUT inversion using a merit function:* Root mean square error (RMSE) between each measured spectrum (i.e. Sentinel-2 data) and modelled (LUT) spectra (Equation 6) was used as a merit function for spectrum matching to find the solution in the LUT.

$$\text{RMSE} = \sqrt{\frac{\sum^{(R_{\text{measured}} - R_{\text{modelled}})} 2}{n}} \tag{6}$$

where $R_{\text{measured}}$ is Sentinel-2 reflectance at wavelength $\lambda$ and $R_{\text{modelled}}$ is simulated reflectance at wavelength $\lambda$ in the LUT, and n is the number of wavelengths.

Darvishzadeh et al. (2008b) proposed an average absolute error threshold value ($\leq 0.02$) between simulated spectra and measured (Sentinel-2) spectra to identify well-simulated bands. We applied this criterion to determine the band subsets used during the retrieval. Therefore, the inversion was carried out using those Sentinel-2 bands found between 650 and 750 nm, which satisfied the criterion and were found in the red and NIR transition zone wavelength range where an increase in chlorophyll content increased absorption. The solution to the inverse problem is the set of input parameters corresponding to the reflectance in the database that provided the smallest RMSE. Because of the potential insufficiency in model formulation and parameterization, and noise related to calibration and pre-processing errors in the observed reflectance, the lowest RMSE might not necessarily provide the best estimates of the solution (Combal et al. 2003). For each measured spectrum, therefore, the first 100 (q) were chosen as potential solutions. From the multiple available solutions (q), the median value was taken as the final solution.

*LUT Inversion using machine learning algorithms*

(i) *Artificial neural network (ANN):* A feed-forward back-propagation neural network with three layers (input, hidden, and output layers) in ©Mathworks was used for this study. The INFORM-simulated spectral dataset, along with the corresponding model input parameters (LCC and LAI) and their derivative (CCC), was divided into three parts of 70%, 15%, and 15%, respectively, for training, validation within the simulated dataset, and testing of the ANN. The training (learning) was initiated with 70% of the LUT dataset to establish

the relationship between the inputs (simulated spectra) and the three outputs (LCC, CCC, and LAI). The performance of the ANN was tested and validated with the remaining data of the LUT before applying the trained network to Sentinel-2 data.

After a series of preliminary tests, the architecture of the neural network was defined to be a single hidden layer with ten nodes and tan-sigmoid transfer function along with three output layers with linear transfer function. The network has been initialized many times to start from different error surfaces. To overcome the overfitting problem of the network and to improve its generalizability, we used early stopping with the scaled conjugate gradient (trainscg) optimization algorithm, which combined the model-trust region approach (used in the Levenberg-Marquardt algorithm) (Moré 1978). Finally, the trained network was used to predict the three variables from the Sentinel-2 L2A spectra and validated using the *in situ* data.

(ii) *Gaussian process regression (GPR):* GPR is becoming one of the alternatives to the state-of-the-art regression methods in predicting biophysical and biochemical parameters from remotely sensed imagery (Pasolli, Melgani, and Blanzieri 2010). GPR is a stochastic Gaussian probability distribution based process, which formulates the learning of the regression by establishing a relation between the input (spectra) and the output (plant traits) variables within a Bayesian framework (Verrelst et al. 2015).

In this study 85% of the INFORM simulated spectral dataset, along with the corresponding model input parameters (LCC and LAI) and their derivative (CCC), was used to train the GPR. The trained GPR was then applied on the INFORM simulated testing dataset and Sentinel-2 L2A spectra. Its performance was evaluated by computing RMSE, RRMSE (%) and bias to assess accuracy, and the coefficient of determination ($R^2$) to account for the goodness-of-fit among the predicted and field measured plant traits. Different kernel functions and prediction methods have been tested. Consequently, the square-exponential function with a subset of data points approximation fit method, and the default block coordinate descent (BCD) prediction method, which provided relatively higher accuracy and $R^2$, was used.

(iii) *Random forest regression (RFR):* RFR is a regression tree based machine learning ensemble first developed by Breiman (2001). It relies on the assumption that overall prediction accuracy can be improved and can control over-fitting by combining different independent predictors (Liang et al. 2016). Many studies demonstrated the higher efficiency of the random forest method compared with the more conventional parametric and linear non-parametric methods (e.g. Mutanga, Adam, and Cho 2012; Vuolo et al. 2013; Liang et al. 2016). RFR training needs setting the number of trees, the number of random features, and the stop criteria. The model was trained by using 85% of the INFORM simulated spectra as predictor and the corresponding input variables (LCC, LAI and CCC) as response data. We used 100 regression trees boosted by the ensemble-aggregation algorithm-LSBoost in Matlab. The grid search method was used to determine the optimal values for the hyperparameters. Three RFR models were run for each of the three response variables. The training process was terminated normally after completing the requested number of training cycles.

(iv) *Stepwise multilinear regression (SMLR):* SMLR fits an observed dependent data set (e.g. LCC, CCC, LAI) using a linear combination of independent variables (e.g. reflectance spectral data at specific bands). The result of this statistical method was that INFORM simulated spectra at a number (N) of wavelengths ($\lambda_i = 1, N$) correlated to the dependent variables.

The stepwise regression was run separately for each of the three variables: LCC, CCC, and LAI. Stepwiselm, a stepwise regression routine in ©Mathworks, was used.

a *Support vector machine learning (SVM):* SVMs were first proposed by Vapnik, Lerner, and Chervone (1965) as a linear classification method and later improved to solve regression problems (Cortes and Vapnik 1995). The basic idea under the SVM method is to transform nonlinear input features into linear regression by defining higher-dimensional space (Hilbert space) (Suykens and Vandewalle 1999; Zeng et al. 2018). Of the INFORM simulated dataset 85% was used for training and the remaining 15% was used for testing in order to examine the performance of different kernel functions and optimization techniques available in the SVM toolbox in Matlab. Finally, the SVM model with fitrsvm iterative support vector machine regression algorithm based on the linear kernel function and sequential minimal optimization (SMO) training method, which is recommended for limited number of predictor variables, was found suitable for our purpose. Thus, this model was trained with the LUT dataset and its performance evaluated using our field data of the three variables.

## 3. Results

The red band (B4) and two red-edge bands (B5 and B6) of Sentinel-2, with central wavelengths of 665, 705, and 740 nm, respectively, showed low absolute error ($\leq 0.02$) between the INFORM simulation and the Sentinel-2 sample plots reflectance data. Thus, training and validation of the machine learning algorithms and inversion of LUT by merit function were performed using a band subset of these three spectral bands. Other band subsets were tested but did not exhibit a strong correlation to the three traits studied and those results have not been reported here.

Figure 1 presents ranges and means values of *in situ* measurements and predictions of the three plant traits. The predicted and *in situ* LCC values fell between 30 and 55 μg/cm$^2$. The CCC values fell in the 0.5–3 g/m$^2$ range, and LAI values ranged between 2 and 6 m$^2$/m$^2$. T-paired tests between *in situ* measurements and predictions (Table 3) did not show a significant difference for many of the tested algorithms. The differences between LCC predictions and *in situ* observations were not significant for any of the methods. However, CCC and LAI predictions by SMLR showed a significant difference with *in situ* observations at $p = 0.05$.

Accuracy assessments using RMSE, RRMSE and Bias for both the testing (INFORM simulated) dataset and validation (*in situ*) dataset have been presented in Table 4 for comparison. Generally, the RRMSE and Bias of the validation result showed a similar trend for many of the methods. All

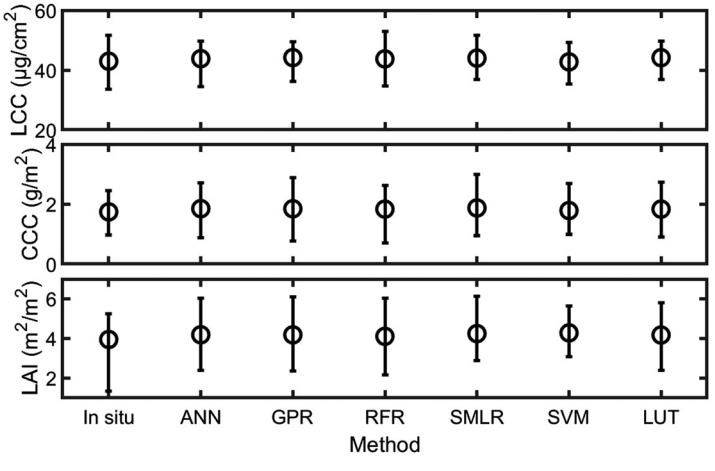


**Figure 1.** Boxplots of range and mean values of *in situ* observations as well as predictions made using six different methods for leaf chlorophyll content (LCC), canopy chlorophyll content (CC), and leaf area index (LAI). The predictions of the LUT method were based on the median of multiple available solutions ($q = 100$).

**Table 3.** Paired *t*-test statistics of traits predicted by different methods against *in situ* observations.

| Trait | Method | *h* | *p* | CI | | stats | sd |
|---|---|---|---|---|---|---|---|
| | | | | lower limit | upper limit | | |
| LCC | ANN | 0 | 0.2634 | −2.4087 | 0.6823 | −1.1391 | 4.2867 |
| | GPR | 0 | 0.0836 | −2.6054 | 0.1713 | −1.7878 | 3.8508 |
| | RFR | 0 | 0.2873 | −2.2365 | 0.6854 | −1.0827 | 4.0520 |
| | SMLR | 0 | 0.1725 | −2.5618 | 0.4795 | −1.3964 | 4.2177 |
| | SVM | 0 | 0.8218 | −1.7568 | 2.1971 | 0.2272 | 5.4800 |
| | LUT | 0 | 0.2315 | −3.1723 | 0.7970 | −1.2204 | 5.5047 |
| CCC | ANN | 1 | **0.0476** | −0.2137 | 0.0012 | −2.0623 | 0.2948 |
| | GPR | 0 | 0.0744 | −0.2190 | 0.0109 | −1.8466 | 0.3187 |
| | RFR | 0 | 0.1412 | −0.2132 | 0.0318 | −1.5000 | 0.3397 |
| | SMLR | 1 | **0.0306** | −0.2482 | 0.0131 | −2.2664 | 0.3261 |
| | SVM | 0 | 0.6255 | −0.2236 | 0.1365 | −0.4930 | 0.4994 |
| | LUT | 0 | 0.1857 | −0.2296 | 0.0464 | −1.3536 | 0.3827 |
| LAI | ANN | 0 | 0.1254 | −0.4738 | 0.0609 | −1.5752 | 0.7415 |
| | GPR | 0 | 0.1342 | −0.4692 | 0.0658 | −1.5379 | 0.7419 |
| | RFR | 0 | 0.3384 | −0.3974 | 0.1408 | −0.9723 | 0.7465 |
| | SMLR | 1 | **0.0446** | −0.5229 | −0.0068 | −2.0933 | 0.7157 |
| | SVM | 1 | **0.0075** | −0.5173 | −0.0868 | −2.8615 | 0.5971 |
| | LUT | 0 | 0.1329 | −0.4484 | 0.0621 | −1.5435 | 0.7080 |

Note: LUT refers to look-up table inversion by merit function, null hypothesis (h = 0), alternative hypothesis (*h* = 1), *p*-value (*p*), 95% confidence interval (CI), T-statistics (stats) and standard deviation (sd). Significant *p* values ($p = 0.05$) are highlighted in bold.

prediction methods exhibited a bias close to zero for the INFORM simulated testing dataset and a slightly negative bias for the *in situ* dataset. ANN provided CCC predictions with the lowest RMSE (0.31 g/m$^2$) for the validation dataset. The SMLR algorithm was fastest in training and predicting the three traits across the whole study area of 1475 × 1510 pixels (Table 4). The LUT inversion took the longest time (36 hrs) on a server computer to map the three traits.

The machine learning predictive models, in general, demonstrated a stronger correlation for the INFOM simulated testing dataset than the *in situ* validation dataset (Table 5). The highest $R^2$ was observed for the INFORM simulated testing dataset of LCC ($R^2 = 0.96$) using ANN, GPR, and

**Table 4.** Root mean square error (RMSE), relative root mean square error (RRMSE) and bias of the six prediction models on the INFORM simulated dataset (INFORM) and the validation dataset (*in situ*) for the three traits: leaf chlorophyll content (LCC), canopy chlorophyll content (CCC) and leaf area index (LAI).

| Method | Accuracy | LCC | | CCC | | LAI | | CPU Time |
|---|---|---|---|---|---|---|---|---|
| | | INFORM | *In situ* | INFORM | *In situ* | INFORM | *In situ* | |
| ANN | RMSE | 3.51 | 4.31 | 0.47 | 0.31 | 1.03 | 0.76 | 20.0 sec |
| | RRMSE | 10.01 | 10.03 | 27.07 | 17.83 | 21.04 | 19.05 | |
| | Bias | 0.01 | −0.86 | 0.00 | −0.11 | 0.00 | −0.21 | |
| GPR | RMSE | 3.52 | 4.25 | 0.46 | 0.33 | 1.01 | 0.74 | 24.8 min. |
| | RRMSE | 10.02 | 9.90 | 26.46 | 19.24 | 20.50 | 18.80 | |
| | Bias | 0.00 | −1.00 | 0.00 | −0.08 | 0.00 | −0.18 | |
| RFR | RMSE | 3.87 | 4.06 | 0.45 | 0.34 | 0.99 | 0.75 | 121.5 sec. |
| | RRMSE | 11.02 | 9.46 | 28.14 | 20.28 | 21.38 | 18.73 | |
| | Bias | −0.01 | −0.78 | 0.00 | −0.13 | 0.01 | −0.13 | |
| SMLR | RMSE | 4.67 | 3.86 | 0.48 | 0.35 | 1.02 | 0.75 | 6.2 sec |
| | RRMSE | 13.33 | 8.86 | 27.67 | 19.93 | 20.76 | 18.90 | |
| | Bias | −0.04 | −0.42 | 0.00 | −0.13 | 0.01 | −0.26 | |
| SVM | RMSE | 3.57 | 4.29 | 0.46 | 0.35 | 1.01 | 0.74 | 24 hrs |
| | RRMSE | 10.16 | 10.00 | 26.52 | 20.67 | 20.52 | 18.83 | |
| | Bias | −0.07 | −1.27 | −0.02 | −0.07 | −0.01 | −0.14 | |
| LUT | RMSE | – | 3.9 | – | 0.33 | – | 0.73 | 36 hrs |
| | RRMSE | – | 9.16 | – | 19.37 | – | 18.16 | |
| | Bias | | −0.69 | | −0.13 | | −0.21 | |

Note: LUT in the method column refers to look-up table inversion by merit function (Equation 2). The time column indicates the elapsed time in training and predicting the three traits for the whole study area. The analysis was performed using a 64 bit processor (Intel® Xeon® CPU ES-2683 v4 @ 2.10 GHz, 512 GB RAM).

**Table 5.** Coefficient of determination ($R^2$) between predictions by the six methods for the testing dataset (INFORM) and the validation dataset (*in situ*). Methods with better performance for each trait are in bold type.

| | LCC | | CCC | | LAI | |
|---|---|---|---|---|---|---|
| Method | INFORM | *In situ* | INFORM | *In situ* | INFORM | *In situ* |
| ANN | 0.96 | 0.26 | 0.79 | **0.66** | 0.42 | **0.43** |
| GPR | 0.96 | 0.26 | 0.79 | 0.62 | 0.45 | 0.45 |
| RFR | 0.95 | **0.34** | 0.77 | 0.**65** | 0.48 | **0.47** |
| SMLR | 0.93 | 0.28 | 0.78 | 0.59 | 0.44 | 0.39 |
| SVM | 0.96 | 0.24 | 0.78 | 0.64 | 0.44 | 0.45 |
| LUT | – | 0.27 | – | **0.65** | – | **0.47** |

SVM. However, when the trained models were applied to the actual image data (Sentinel-2), the predicted against the validation values portrayed a weaker correlation for LCC than for the other two traits, CCC and LAI. The validation results of RFR elicited relatively higher $R^2$ for all three plant traits: LCC ($R^2 = 0.34$), CCC ($R^2 = 0.65$), and LAI ($R^2 = 0.47$). The LUT inversion by merit function showed similar performance to RFR, especially for CCC and LAI.

Scatter plots that compare predictions obtained by RFR and the *in situ* measured values of the three traits are presented in Figure 2. As can be observed from the figure, the prediction was more precise for LCC (RRMSE = 9.46%) than for CCC (RRMSE = 20.48%) and LAI (RRMSE = 18.73%), although the inverse is true for correlation. There was no tendency of under/overestimation, and predicted values were scattered closely around the 1:1 relationship lines for all three traits.

## 4. Discussion and conclusion

Our study was designed to determine the effective INFORM inversion approach to retrieve LCC, CCC, and LAI from Sentinel-2 top of canopy reflectance data. The results of this study indicated that machine learning algorithms, which are flexible and computationally efficient, can predict the three biodiversity traits (i.e. LCC, CCC, and LAI) with accuracies comparable to the generic but computationally expensive LUT based INFORM inversion using merit function (Table 4).

Contrary to expectations, this study found generally higher RMSE for the INFORM simulated dataset than the *in situ* validation dataset, particularly for CCC and LAI (Table 4). A possible reason could be that the variability in the INFORM simulated dataset was higher than the variability in the validation dataset. To ensure a thorough test of the accuracy and robustness of predictive models, the INFORM dataset was simulated with a wide range of variability (Figure 2).

The most prominent finding to emerge from this study was that many of the tested inversion algorithms yielded a relationship and accuracy of prediction that was similar for *in situ* and modelled values regarding the three biodiversity traits. In general, LCC was retrieved with higher precision

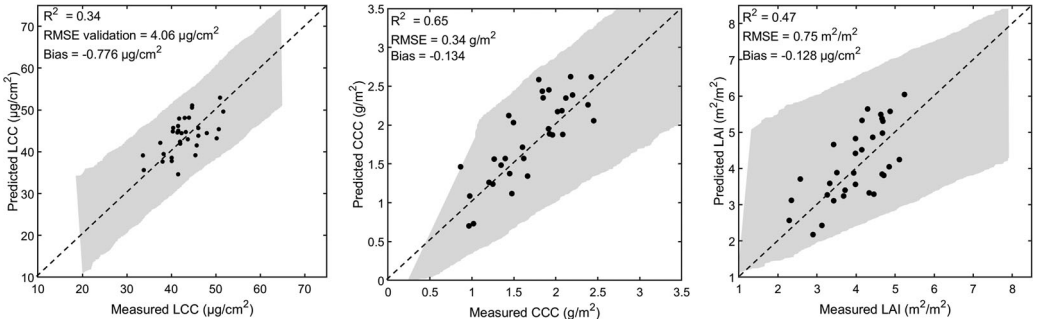


**Figure 2.** Scatterplots of estimated versus measured leaf chlorophyll content (LCC), canopy chlorophyll content (CCC), and leaf area index (LAI) yielded by inversion of INFORM using the RFR method. Broken lines show the one-to-one relationship, and shaded areas illustrate the range of the INFORM input parameter dataset and the corresponding prediction by RFR.

(RRMSE) than the other two traits (Table 4). A possible explanation for this could be the higher number of uncertainties in the *in situ* measurements of LAI (also indirectly affecting CCC) than of LCC. Our findings were in agreement with the previous study by Verrelst et al. (2012), who obtained a RRMSE of 7.1% and 23% for LCC and LAI, respectively, using a GPR algorithm on simulated Sentinel-2 data. The lowest RMSE observed for LCC (RMSE = 3.86 μg/cm$^2$) in our study were far below those observed by Darvishzadeh et al. (2019), who obtained a RMSE of 8.6 μg/cm$^2$ by inversion of the INFORM model in the same study area using LUT based merit function. This discrepancy could be attributed to INFORM parameterization. Darvishzadeh et al. (2019) used 500,000 LUT entries with a uniform distribution. Whereas, in this study, leaf and canopy level input parameters were determined using a multivariate normal distribution function, which maintained the actual relationship between input variables and thus removed unrealistic input variable combinations that could have decreased accuracy. Another possible explanation could be that the field data used in (Darvishzadeh et al. 2019) included only spruce samples, while we used samples from both broadleaf and conifer stands. The uncertainties in measuring *in situ* chlorophyll might be higher in conifer needles than in broadleaf leaves.

However, the explained variance ($R^2$) between predicted and *in situ* measurement was lower for LCC ($R^2 = 0.34$) than CCC ($R^2 = 0.66$) and LAI ($R^2 = 0.47$) (Table 4). These results reflected those of Liang et al. (2016), who found an $R^2$ of 0.77 for CCC and an $R^2$ of only 0.33 for LCC inversion from hyperspectral remote sensing data in crop fields. Darvishzadeh et al. (2019) achieved the slightly higher $R^2$ of 0.39 in predicting LCC in the same study area. It is, therefore, likely that lower RMSE and higher $R^2$ combinations may not always exist.

Among the tested algorithms, RFR validation provided relatively higher $R^2$ and lower RMSE combinations for all three traits compared to the performance of LUT inversion by merit function (Tables 4 and 5). This finding suggests that the radiative transfer model inversion using machine learning regression algorithms is a robust and fast approach when predicting biodiversity variables of terrestrial surfaces from remote sensing data. The present results are significant in at least two respects. One of the benefits is that the training of the algorithms is based on RTM simulation, and thus, field measurements are only required for validation. Also, the trained algorithms are equipped with the generic capability of RTMs and the simplicity of statistical approaches that overcome the transferability, space, and time-specific limitations of statistical models in large scale mapping of plant traits from remote sensing data.

In our study, both the LUT inversion using merit function and the machine learning algorithms revealed a similar precision in predicting LAI (Table 4). The LUT inversion using the merit function produced marginally better accuracy (RMSE = 0.73 m$^2$/m$^2$) than the machine learning algorithms (0.74–0.76 m$^2$/m$^2$), which did not show significant differences during the paired t-test. This finding is contrary to that of Atzberger et al. (2015). The latter found significantly lower accuracy (RMSE = 1.1 m$^2$/m$^2$) when training second-order polynomial function on the PROSAIL RTM synthetic data than when training LUT inversion by merit function (RMSE = 0.53 m$^2$/m$^2$) to retrieve LAI of Mediterranean grassland from airborne imaging spectroscopy. A possible explanation for these contradicting results could stem from generating the LUT. RTM input parameters are naturally cross-correlated (Ali et al. 2016b), and it is imperative to consider such correlation in parameterizing RTMs and to generate LUTs. Neglecting such relationships may not affect LUT inversion by merit function since the solution is found by searching matching spectra, but could profoundly affect the performance of fitting equations, which depend on the relationship between input parameter and simulated spectra. We used a multivariate normal distribution function based on the mean and covariance matrix of *in situ* data in parametrizing the RTM, whereas Atzberger et al. (2015) generated their LUT using the random distribution of model input parameters. Hence, it could conceivably be hypothesized that RTM inversions can be performed interchangeably by machine learning regression algorithms and LUT inversion by merit function, as long as the natural relationships between input parameters are maintained during RTM parameterization. Besides, preserving relationships between input parameters during LUT generation helps to circumvent ill-posed

problems, since they minimize the chance of having unrealistic combinations of input parameters that may result in multiple similar spectra.

A paired *t-test* of the predictions made by the machine learning methods, particularly RFR and GPR, did not show a statistical difference with the corresponding *in situ* measurements of the three traits (Figure 1 and Table 3). The predictions were unbiased and did not exhibit any tendency to over/underestimate, as can be seen in Figure 2. This further supports our conclusion that training machine learning regression methods using synthetic data can yield results that are as generic as LUT inversion by merit function, and can confidently be used for large scale mapping of vegetation properties from remote sensing data.

In broad terms, our findings have showcased the potential of machine learning algorithms trained on the INFORM simulated dataset to fast and accurately predict plant traits from Sentinel-2 data. We examined the predictability of the three traits in mixed temperate forests. Further work is required to establish the viability of the proposed methods in different vegetation types and for other plant traits.

## Disclosure statement

No potential conflict of interest was reported by the author(s).

## ORCID

*Abebe Mohammed Ali* http://orcid.org/0000-0002-3962-0333
*Roshanak Darvishzadeh* http://orcid.org/0000-0001-7512-0574
*Andrew Skidmore* http://orcid.org/0000-0002-7446-8429
*Tawanda W. Gara* http://orcid.org/0000-0001-8134-4849
*Marco Heurich* http://orcid.org/0000-0003-0051-2930

## References

Ali, A. M., R. Darvishzadeh, A. Skidmore, T. W. Gara, B. O'Connor, C. Roeoesli, M. Heurich, and M. Paganini. 2020. "Comparing Methods for Mapping Canopy Chlorophyll Content in a Mixed Mountain Forest Using Sentinel-2 Data." *International Journal of Applied Earth Observation and Geoinformation* 87: 102037.

Ali, A. M., R. Darvishzadeh, A. K. Skidmore, I. van Duren, U. Heiden, and M. Heurich. 2016a. "Estimating Leaf Functional Traits by Inversion of PROSPECT: Assessing Leaf dry Matter Content and Specific Leaf Area in Mixed Mountainous Forest." *International Journal of Applied Earth Observation and Geoinformation* 45: 66–76.

Ali, A. M., A. K. Skidmore, R. Darvishzadeh, I. van Duren, S. Holzwarth, and J. Mueller. 2016b. "Retrieval of Forest Leaf Functional Traits from HySpex Imagery Using Radiative Transfer Models and Continuous Wavelet Analysis." *ISPRS Journal of Photogrammetry and Remote Sensing* 122: 68–80.

Asner, G. P. 1998. "Biophysical and Biochemical Sources of Variability in Canopy Reflectance." *Remote Sensing of Environment* 64: 234–253.

Atzberger, C. 2000. "Development of an Invertible Forest Reflectance Model: The INFOR-Model." In *Proceedings of the 20th EARSeL Symposium*, edited by M. F. Buchroithner, 39–44. Dresden, Germany: Decade of Trans-European Remote Sensing Cooperation.

Atzberger, C., R. Darvishzadeh, M. Immitzer, M. Schlerf, A. Skidmore, and G. le Maire. 2015. "Comparative Analysis of Different Retrieval Methods for Mapping Grassland Leaf Area Index Using Airborne Imaging Spectroscopy." *International Journal of Applied Earth Observation and Geoinformation* 43: 19–31.

Atzberger, C., R. Darvishzadeh, M. Schlerf, and G. Le Maire. 2013. "Suitability and Adaptation of PROSAIL Radiative Transfer Model for Hyperspectral Grassland Studies." *Remote Sensing Letters* 4: 56–65.

Baret, F. 2016. *S2ToolBox Level 2 Products: LAI, FAPAR, FCOVER*. Avignon, France: INRA.

Breiman, L. 2001. "Random Forests." *Machine Learning* 45: 5–32.

Broge, N. H., and J. V. Mortensen. 2002. "Deriving Green Crop Area Index and Canopy Chlorophyll Density of Winter Wheat From Spectral Reflectance Data." *Remote Sensing of Environment* 81: 45–57.

Cailleret, M., M. Heurich, and H. Bugmann. 2014. "Reduction in Browsing Intensity may not Compensate Climate Change Effects on Tree Species Composition in the Bavarian Forest National Park." *Forest Ecology and Management* 328: 179–192.

Clevers, J. G. P. W., L. Kooistra, and M. M. M. van den Brande. 2017. "Using Sentinel-2 Data for Retrieving LAI and Leaf and Canopy Chlorophyll Content of a Potato Crop." *Remote Sensing* 9 (5): 1–15.

Combal, B., F. Baret, M. Weiss, A. Trubuil, D. Mace, A. Pragnere, R. Myneni, Y. Knyazikhin, and L. Wang. 2003. "Retrieval of Canopy Biophysical Variables from Bidirectional Reflectance – Using Prior Information to Solve the Ill-posed Inverse Problem." *Remote Sensing of Environment* 84: 1–15.

Cortes, C., and V. Vapnik. 1995. "Support-vector Networks." *Machine Learning* 20: 273–297.

Darvishzadeh, R., A. Skidmore, H. Abdullah, E. Cherenet, A. Ali, T. Wang, W. Nieuwenhuis, et al. 2019. "Mapping Leaf Chlorophyll Content from Sentinel-2 and RapidEye Data in Spruce Stands Using the Invertible Forest Reflectance Model." *International Journal of Applied Earth Observation and Geoinformation* 79: 58–70.

Darvishzadeh, R., A. Skidmore, C. Atzberger, and S. van Wieren. 2008a. "Estimation of Vegetation LAI from Hyperspectral Reflectance Data: Effects of Soil Type and Plant Architecture." *International Journal of Applied Earth Observation and Geoinformation* 10: 358–373.

Darvishzadeh, R., A. Skidmore, M. Schlerf, and C. Atzberger. 2008b. "Inversion of a Radiative Transfer Model for Estimating Vegetation LAI and Chlorophyll in a Heterogeneous Grassland." *Remote Sensing of Environment* 112: 2592–2604.

Drusch, M., U. Del Bello, S. Carlier, O. Colin, V. Fernandez, F. Gascon, B. Hoersch, et al. 2012. "Sentinel-2: ESA's Optical High-Resolution Mission for GMES Operational Services." *Remote Sensing of Environment* 120: 25–36.

Féret, J. B., C. François, A. Gitelson, G. P. Asner, K. M. Barry, C. Panigada, Andrew D. Richardson, and S. Jacquemoud. 2011. "Optimizing Spectral Indices and Chemometric Analysis of Leaf Chemical Properties Using Radiative Transfer Modeling." *Remote Sensing of Environment* 115: 2742–2750.

Féret, J. B., G. le Maire, S. Jay, D. Berveiller, R. Bendoula, G. Hmimina, A. Cheraiet, et al. 2018. "Estimating Leaf Mass Per Area and Equivalent Water Thickness Based on Leaf Optical Properties: Potential and Limitations of Physical Modeling and Machine Learning." *Remote Sensing of Environment* 231: 110959-1–110959-14.

Gamon, J. A., B. Somers, Z. Malenovsky, E. M. Middleton, U. Rascher, and M. E. Schaepman. 2019. "Assessing Vegetation Function with Imaging Spectroscopy." *Surveys in Geophysics* 40: 489–513.

Gara, T. W., R. Darvishzadeh, A. K. Skidmore, T. Wang, and M. Heurich. 2019. "Accurate Modelling of Canopy Traits from Seasonal Sentinel-2 Imagery Based on the Vertical Distribution of Leaf Traits." *ISPRS Journal of Photogrammetry and Remote Sensing* 157: 108–123.

Heurich, M., B. Beudert, H. Rall, and Z. Křenová. 2010. "National Parks as Model Regions for Interdisciplinary Long-Term Ecological Research: The Bavarian Forest and Šumavá National Parks Underway to Transboundary Ecosystem Research." In *Long-Term Ecological Research: Between Theory and Application*, edited by F. Müller, C. Baessler, H. Schubert, and S. Klotz, 327–344. Dordrecht: Springer Netherlands.

Holloway, J., and K. Mengersen. 2018. "Statistical Machine Learning Methods and Remote Sensing for Sustainable Development Goals: A Review." *Remote Sensing* 10: 1365.

Houborg, R., J. B. Fisher, and A. K. Skidmore. 2015. "Advances in Remote Sensing of Vegetation Function and Traits." *International Journal of Applied Earth Observation and Geoinformation* 43: 1–6.

Houborg, R., H. Soegaard, and E. Boegh. 2007. "Combining Vegetation Index and Model Inversion Methods for the Extraction of Key Vegetation Biophysical Parameters Using Terra and Aqua MODIS Reflectance Data." *Remote Sensing of Environment* 106: 39–58.

Huemmrich, K. F. 2001. "The GeoSail Model: A Simple Addition to the SAIL Model to Describe Discontinuous Canopy Reflectance." *Remote Sensing of Environment* 75: 423–431.

Jacquemoud, S., and F. Baret. 1990. "Prospect – A Model of Leaf Optical-Properties Spectra." *Remote Sensing of Environment* 34: 75–91.

Jacquemoud, S., W. Verhoef, F. Baret, C. Bacour, P. J. Zarco-Tejada, G. P. Asner, C. François, and S. L. Ustin. 2009. "PROSPECT Plus SAIL Models: A Review of Use for Vegetation Characterization." *Remote Sensing of Environment* 113: S56–S66.

Lehnert, L. W., C. Bassler, R. Brandl, P. J. Burton, and J. Muller. 2013. "Conservation Value of Forests Attacked by Bark Beetles: Highest Number of Indicator Species is Found in Early Successional Stages." *Journal for Nature Conservation* 21: 97–104.

Liang, L., Z. Qin, S. Zhao, L. Di, C. Zhang, M. Deng, H. Lin, L. Zhang, L. Wang, and Z. Liu. 2016. "Estimating Crop Chlorophyll Content with Hyperspectral Vegetation Indices and the Hybrid Inversion Method." *International Journal of Remote Sensing* 37: 2923–2949.

Malenovský, Z., E. Martin, L. Homolová, J.-P. Gastellu-Etchegorry, R. Zurita-Milla, M. E. Schaepman, R. Pokorny, J. Clevers, and P. Cudlín. 2008. "Influence of Woody Elements of a Norway Spruce Canopy on Nadir Reflectance Simulated by the DART Model at Very High Spatial Resolution." *Remote Sensing of Environment* 112: 1–18.

Moré, J. J. 1978. "The Levenberg-Marquardt Algorithm: Implementation and Theory." *Numerical Analysis* 630: 105–116.

Mutanga, O., E. Adam, and M. A. Cho. 2012. "High Density Biomass Estimation for Wetland Vegetation Using WorldView-2 Imagery and Random Forest Regression Algorithm." *International Journal of Applied Earth Observation and Geoinformation* 18: 399–406.

Myneni, R. B., R. Ramakrishna, R. Nemani, and S. W. Running. 1997. "Estimation of Global Leaf Area Index and Absorbed par Using Radiative Transfer Models." *IEEE Transactions on Geoscience and Remote Sensing* 35: 1380–1393.

Pasolli, L., F. Melgani, and E. Blanzieri. 2010. "Gaussian Process Regression for Estimating Chlorophyll Concentration in Subsurface Waters from Remote Sensing Data." *Ieee Geoscience and Remote Sensing Letters* 7: 464–468.

Pasqualotto, N., J. Delegido, S. Van Wittenberghe, M. Rinaldi, and J. Moreno. 2019. "Multi-Crop Green LAI Estimation with a New Simple Sentinel-2 LAI Index (SeLI)." *Sensors (Basel, Switzerland)* 19: 904.

Pereira, H. M., S. Ferrier, M. Walters, G. N. Geller, R. H. G. Jongman, R. J. Scholes, M. W. Bruford, et al. 2013. "Essential Biodiversity Variables." *Science* 339: 277–278.

Rosema, A., W. Verhoef, H. Noorbergen, and J. J. Borgesius. 1992. "A New Forest Light Interaction-model in Support of Forest Monitoring." *Remote Sensing of Environment* 42: 23–41.

Schlerf, M., and C. Atzberger. 2006. "Inversion of a Forest Reflectance Model to Estimate Structural Canopy Variables from Hyperspectral Remote Sensing Data." *Remote Sensing of Environment* 100: 281–294.

Skidmore, A. K. 2002. "Taxonomy of Environmental Models in the Spatial Sciences." In *Environmental Modelling with GIS and Remote Sensing*, edited by A. Skidmore, 8–24. London: Taylor & Francis.

Skidmore, A. K., N. Pettorelli, N. C. Coops, G. N. Geller, H. Hansen, R. Lucas, C. A. Mücher, et al. 2015. "Agree on Biodiversity Metrics to Track from Space." *Nature* 523: 403–405.

Suykens, J. A. K., and J. Vandewalle. 1999. "Least Squares Support Vector Machine Classifiers." *Neural Processing Letters* 9: 293–300.

Thenkabail, P. S., R. B. Smith, and E. De Pauw. 2000. "Hyperspectral Vegetation Indices and their Relationships with Agricultural Crop Characteristics." *Remote Sensing of Environment* 71: 158–182.

Vapnik, V. N., A. Y. Lerner, and Ay Chervone. 1965. "Learning Systems for Pattern Recognition Using Generalized Portraits." *Engineering Cybernetics* 24 (6): 774–780.

Verhoef, W. 1984. "Light-Scattering by Leaf Layers with Application to Canopy Reflectance Modeling – the Sail Model." *Remote Sensing of Environment* 16: 125–141.

Verrelst, J., G. Camps-Valls, J. Muñoz-Marí, J. P. Rivera, F. Veroustraete, J. G. P. W. Clevers, and J. Moreno. 2015. "Optical Remote Sensing and the Retrieval of Terrestrial Vegetation Bio-geophysical Properties – A Review." *ISPRS Journal of Photogrammetry and Remote Sensing* 108: 273–290.

Verrelst, J., J. Muñoz, L. Alonso, J. Delegido, J. P. Rivera, G. Camps-Valls, and J. Moreno. 2012. "Machine Learning Regression Algorithms for Biophysical Parameter Retrieval: Opportunities for Sentinel-2 and −3." *Remote Sensing of Environment* 118: 127–139.

Verrelst, J., M. E. Schaepman, Z. Malenovský, and J. G. P. W. Clevers. 2010. "Effects of Woody Elements on Simulated Canopy Reflectance: Implications for Forest Chlorophyll Content Retrieval." *Remote Sensing of Environment* 114: 647–656.

Vuolo, F., C. Atzberger, K. Richter, G. D'Urso, and J. Dash. 2010. "Retrieval of Biophysical Vegetation Products from Rapideye Imagery." *100 Years Isprs Advancing Remote Sensing Science, Pt 1* 38: 281–286.

Vuolo, F., N. Neugebauer, S. F. Bolognesi, C. Atzberger, and G. D'Urso. 2013. "Estimation of Leaf Area Index Using DEIMOS-1 Data: Application and Transferability of a Semi-Empirical Relationship between Two Agricultural Areas." *Remote Sensing* 5: 1274–1291.

Wang, K., S. E. Franklin, X. L. Guo, and M. Cattet. 2010. "Remote Sensing of Ecology, Biodiversity and Conservation: A Review from the Perspective of Remote Sensing Specialists." *Sensors* 10: 9647–9667.

Wang, Z., A. K. Skidmore, T. Wang, R. Darvishzadeh, U. Heiden, M. Heurich, and J. Hearne. 2017. "Canopy Foliar Nitrogen Retrieved from Airborne Hyperspectral Imagery by Correcting for Canopy Structure Effects." *International Journal of Applied Earth Observation and Geoinformation* 54: 84–94.

Widlowski, J.-L., C. Mio, M. Disney, J. Adams, I. Andredakis, C. Atzberger, J. Brennan, et al. 2015. "The Fourth Phase of the Radiative Transfer Model Intercomparison (RAMI) Exercise: Actual Canopy Scenarios and Conformity Testing." *Remote Sensing of Environment* 169: 418–437.

Yanez-Rausell, L., Z. Malenovsky, M. Rautiainen, J. G. P. W. Clevers, P. Lukes, J. Hanus, and M. E. Schaepman. 2015. "Estimation of Spruce Needle-Leaf Chlorophyll Content Based on DART and PARAS Canopy Reflectance Models." *IEEE Journal of Selected Topics in Applied Earth Observations and Remote Sensing* 8 (4): 1–9.

Zeng, W. Z., D. Y. Zhang, Y. H. Fang, J. W. Wu, and J. S. Huang. 2018. "Comparison of Partial Least Square Regression, Support Vector Machine, and Deep-Learning Techniques for Estimating Soil Salinity from Hyperspectral Data." *Journal of Applied Remote Sensing* 12 (2): 022204-1–022204-16. doi:10.1117/1.JRS.12.022204.